Unimolecular decomposition in the sputtering of metal clusters

A. Wucher
Fachbereich Physik der Universität Kaiserslautern, D-6750 Kaiserslautern, Federal Republic of Germany

B. J. Garrison
Department of Chemistry, Pennsylvania State University, University Park, Pennsylvania 16802
(Received 13 November 1991; revised manuscript received 28 February 1992)

The stability of metal clusters M_n sputtered from single-crystal surfaces by keV and sub-keV Ar^+ ions was investigated by a molecular-dynamics (MD) simulation using a many-body embedded-atom potential. It is shown that the clusters identified within the sputtered flux immediately after the ion impact contain an average internal energy of roughly 1 eV per constituent atom. Consequently, most of the sputtered trimers and tetramers and virtually all ejected clusters with $n \geq 5$ are found to be unstable and therefore decompose into stable fragments on a time scale of several tens of picoseconds after the ejection. The contribution of fragmentation to the yields, translational and internal energy distributions of stable and, hence, experimentally detectable dimers, trimers, and tetramers were calculated. It is found that this contribution increases strongly with increasing primary-ion energy E_B and becomes comparable to the contribution of "intrinsic" stable molecules (i.e., such molecules that are identified immediately after the sputtering process) at $E_B = 5$ keV. It is shown that the experimental data available on Ag_n multimers sputtered from polycrystalline silver can be reproduced very well by the MD simulation if fragmentation processes are included in predicting the yields and distributions.

I. INTRODUCTION

When a solid is bombarded with energetic ions, a variety of particles is ejected from the solid. This process is usually called sputtering. It has been long known that especially for clean metallic surfaces an abundant fraction of the sputtered flux may be ejected as agglomerations of two or more atoms. The kinetics leading to the formation of these sputtered clusters have been the subject of a long-standing discussion in the literature. Several statistical models have been proposed describing the formation of sputtered molecules either as an ejection of the molecule as a whole or as a combination of individually sputtered atoms subsequent to the ejection process.[1–14] Both types of models suffer from the fact that the formation of a sputtered molecule requires a highly correlated ejection of the constituent atoms which is difficult to describe by any statistical means. An approach which circumvents this problem is given by molecular-dynamics simulations (MDS) of the collision cascade leading to the ejection of sputtered particles. Consequently, a large number of MDS studies have been devoted to the formation of clusters during sputtering.[15–24] A fairly recent review of this work can be found in Ref. 25. As pointed out in this paper, however, the MDS investigations published to date suffer from two major shortcomings. First, the exclusive use of additive pair potentials describing the interaction between target atoms precluded an accurate description of the solid material and gas-phase clusters *at the same time.* Hence, the need to switch from a "solid" to a "gas-phase" interaction potential at some stage during the ejection process is introduced. Second, sputtered clusters containing more than two atoms may undergo unimolecular fragmentation if they contain an internal energy which is above the dissociation threshold. Depending on the time scale of these processes, the numbers of sputtered clusters reported "immediately after the ejection process" may be significantly altered or even become meaningless. To date, however, the effect of unimolecular decomposition has not been included into the molecular-dynamics (MD) treatment of cluster sputtering. In the present paper, we try to tackle both problems mentioned above by (a) using a many-body potential constructed by the embedded-atom method (EAM) to describe the atom-atom interaction both within the solid *and* the in gas phase and (b) carrying the simulation on until all unstable clusters have decomposed into stable fragments. The success of both attempts will be largely determined by the quality of the interaction potential used. From the work of Garrison and co-workers[26] it has been definitively shown that the EAM potentials are currently the best ones available for use in MD simulations of keV particle bombardment of fcc metals. To examine the physical relevance of these potentials to small homonuclear metal clusters, we determine in a first step the basic properties of such clusters (like geometrical structure, binding energies, etc.) which are given by an EAM potential. In order to establish some link to experimental data, we use a potential specifically designed for silver which was shown previously to work very well in MD simulations of Ag atom and Ag_2 dimer sputtering.[27,28]

II. DESCRIPTION OF THE CALCULATION

The molecular-dynamics simulation has been described in great detail earlier.[26,29] In short, the classical equa-

tions of motion are solved numerically for all atoms of a crystallite containing approximately 1000 metal atoms. While the interaction between the impinging Ar^+ ion and the metal atoms was described by a conventional pairwise additive potential of the Moliere type,[30] a many-body potential constructed by the EAM was used to describe the interaction between target atoms. In the EAM the potential energy of the ith atom is written as $V_i = F[\rho_i = \sum_{i \neq j} \rho_{\text{atomic}}(r_{ij})] + \frac{1}{2}\sum_{i \neq j} \phi(r_{ij})$. In this expression, r_{ij} is the distance between the ith and jth atoms, $\rho_{\text{atomic}}(r_{ij})$ is the electron density at the position of the ith atom due to the jth atom, and ρ_i is the total electron density at the position of the ith atom. In the present study, we use a potential which was originally fitted by Foiles, Baskes, and Daw[31] to experimental data of solid silver. As described in detail elsewhere,[28] the potential was modified to include a sufficiently repulsive interaction at small internuclear separations. The reason for choosing this particular EAM potential was that we want to compare some of the results obtained from the simulation to a relatively large set of experimental data available on the sputtering of small Ag_n clusters by keV Ar^+ bombardment of silver surfaces.[32,33] It should be emphasized at this point, however, that the present study is devoted to the investigation of sputtered metal clusters in a more general manner and that the EAM potential used throughout this study should be considered as a model potential describing an arbitrary fcc metal rather than as an accurate description of silver. In order to document this, we will in the following use the symbol M_n, which denotes a homonuclear metal cluster consisting of n atoms, where M stands for a generic metal.

The identification and classification of sputtered clusters was done as follows. First, the list of sputtered atoms obtained for a given primary-ion impact was examined for bound atom pairs. In this context, a pair of atoms was considered bound if its total energy given by the sum of the potential (V) and kinetic energy relative to the center of mass (E_r) of both atoms was less than zero. Then, the resulting list of atom pairs was scanned for linked or overlapping bonds and the largest possible cluster size was determined. A "candidate" cluster determined this way was subjected to a first stability check by calculating its total energy

$$E_{\text{tot}}^{\text{cluster}} = \sum_{i=1}^{n} E_i^{\text{rel}} + V_i \ . \tag{1}$$

Here, n is the number of atoms in the candidate cluster, E_i^{rel} is the kinetic energy of the ith atom in the center-of-mass system of the cluster, and V_i denotes the EAM potential energy calculated for the ith atom as described above. If E_{tot} was determined to be less than zero, this group of atoms was considered to be an ejected cluster. Up to this point, the procedure is completely analogous to the cluster detection scheme applied in earlier MDS work using pair potentials.[15–17] The situation now is that at the time the integration of the collision cascade was stopped, i.e., at in general several hundred femtoseconds after the primary-ion impact, we have an M_n cluster among the flux of sputtered particles which contains less internal energy E_{int} than its atomization energy and, hence, cannot decompose into n single atoms. The next step is then to determine whether this cluster is absolutely stable or metastable, i.e., whether E_{int} is below or above the dissociation threshold E_d of the cluster. In order to obtain E_d, on the other hand, the atomization energy E_a of M_n clusters due to the EAM potential has to be known as a function of the cluster size n. The quantity $E_a(n)$ can be determined by finding the minimum energy configuration of atoms using the EAM potential. For the small cluster sizes of interest here this is accomplished easily by assuming a geometry for the n atoms and then performing a molecular-dynamics calculation where a frictional force is included on each atom in order to remove excess kinetic energy. Ultimately the atoms reach a configuration corresponding to the local minimum of the EAM potential hypersurface which is closest to the starting geometry. In order to make sure that a *global* potential minimum is found, several trial geometries were used. The atomization energy $E_a(n)$ was set equal to the total potential energy in the lowest-lying minimum. It is of note that although this procedure does not guarantee that the absolute potential minimum is found, in particular for the clusters with $n \geq 5$, the energy difference between the various local minima determined for a given cluster was small and the resulting possible error of E_a is only of the order of several percent.

From the cluster atomization energies, the energy thresholds $E_{\text{th}}^{(m)}$ for the unimolecular decomposition reactions given by

$$M_n \xrightarrow{E_{\text{th}}^{(m)}} M_{n-m} + M_m \quad (m = 1, \ldots, n-1) \tag{2}$$

were calculated as

$$E_{\text{th}}^{(m)} = E_a(n-m) + E_a(m) - E_a(n) \ . \tag{3}$$

The lowest value of $E_{\text{th}}^{(m)}$ determines the dissociation threshold E_d of the M_n cluster. A sputtered cluster was considered to be stable if its internal energy was less than E_d. All other clusters identified by the procedure described above were considered to be unstable and, hence, subject to dissociation. In order to allow a comparison of calculated cluster yields with corresponding experimental data, it is of interest to estimate the lifetime of these unstable clusters, because most experimental schemes make the cluster identification at times of at least several microseconds after the ejection event. Hence, if an unstable cluster has a lifetime greater than this it will be detected the same as a stable cluster. If, on the other hand, the lifetime is shorter, then smaller clusters and atoms will be detected. Numerous methods are available for estimating lifetimes, but since we have the positions and velocities of the atoms in each unstable cluster, we used the molecular-dynamics approach to determine the lifetimes. In other words, the numerical integration of the equations of motion was continued for the constituent atoms of an unstable cluster. (For computational efficiency we do this in a modified version of the MDS code so that we can omit all the other atoms.) The limitation of this MDS procedure is that the atomic motions can only be

followed for nanoseconds before computer roundoff errors interfere. However, for most of the unstable clusters found in these simulations, this was shown not to be a severe constraint. To quantitatively estimate the lifetimes, the cluster definition discussed above was reapplied periodically during the numerical integration. The first occurrence of the unstable cluster M_n dissociating into smaller stable or unstable subclusters was recorded as the *dissociation lifetime* τ of the sputtered cluster. The trajectory integration, however, was continued until only stable subclusters were detected. The time elapsed until this condition was reached was called the *decomposition time* t_d of the cluster and the properties of the stable fragments were stored. In order to limit the computation time, an upper time boundary of 200 ps was set after which the integration was stopped even if the stopping condition was not found. As discussed in Sec. III, however, only in the case of sputtered trimers and tetramers with internal energies extremely close to the dissociation threshold this limitation played a non-negligible role.

In order to investigate the role of the primary-ion energy E_B with respect to the formation and dissociation of sputtered clusters, simulations were performed for Ar^+ ions normally incident onto a (111) surface employing various values of E_B between 250 eV and 5 keV. Furthermore, the influence of the nature of the bombarded surface was studied by running additional simulations for 1-keV Ar^+ impinging onto (110) and (100) surfaces as well. A total of 1000 trajectories (equal to primary-ion impacts) were run for each of these simulations. The impact points were chosen to be uniformally distributed over the smallest irreducible cell of the surface under investigation.

III. RESULTS AND DISCUSSION

Following the procedures outlined above, this section is organized into five subsections. In Sec. III A the equilibrium cluster geometries obtained from the EAM potential are presented and the threshold energy for dissociation is evaluated as a function of the cluster size. In Sec. III B the internal energy distribution of those clusters which are identified immediately after the sputtering event is described and the numbers of stable and unstable clusters of each size are determined. Sections III C and III D then deal with the dissociation of the unstable clusters and their decomposition into stable fragments, respectively. Finally, in Sec. III E the influence of fragmentation on the yields as well as the internal and translational energy distribution of sputtered clusters is discussed.

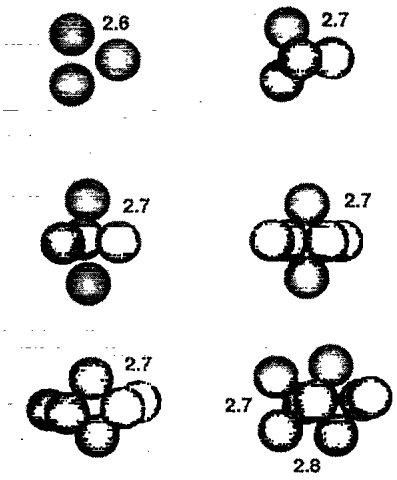

FIG. 1. Equilibrium geometry of M_n microclusters with $n=3,\ldots,8$ according to the embedded-atom (EAM) potential described in the text. The numbers given in the figure denote the calculated bond lengths in Å units.

A. Equilibrium cluster geometry and atomization energies

Figure 1 shows the geometry of M_n clusters with $n=2,\ldots,8$ which was determined to be most stable according to the EAM interaction potential. The equilibrium configurations obtained here reflect the spherical symmetry of the EAM potential and thus do not include subtle effects like Jahn-Teller distortion. The somewhat interesting configuration of M_8 displayed in Fig. 1 looks very similar to the one obtained by Röthlisberger and Andreoni for Na_8 (see Fig. 4a in Ref. 34).

The atomization energies of the different clusters which were calculated from the configurations shown in Fig. 1 are given in Table I. Since the EAM potential used

TABLE I. Atomization energies of M_n clusters with $n=2,\ldots,8$ as determined from the EAM potential. For comparison, corresponding theoretical and experimental values given for Ag_n clusters (taken from the references given in the second row) are included. Values are given in eV.

Present calculation EAM	Ag_n literature data Theor.						Expt.
	Ref. 35	Ref. 36	Ref. 37	Ref. 38	Ref. 39	Ref. 40	Ref. 41
M_2 2.63	1.62	1.64		1.57	1.66	1.82	1.66
M_3 4.82	2.40	2.27	2.32	2.64	1.05	2.76	2.55
M_4 7.24	4.44	3.81		7.19	1.90	2.52	
M_4 9.55	6.10				2.78	5.28	
M_6 11.96					3.82	5.28	
M_7 14.34				4.56	7.42		
M_8 16.58						9.44	

was originally designed for silver (cf. Sec. II), corresponding values obtained for small silver clusters from recent *ab initio* calculations and, for the case of Ag_2 and Ag_3, experimental results are also included in the table. It is obvious that in all cases the EAM potential yields binding energies which are by factors between 1.5 and 2.0 higher than the theoretical or experimental values given for the corresponding Ag_n. As a consequence, care must be taken when comparing the results calculated in the present study to experimental data obtained for sputtered Ag_n clusters. The implication of this will be discussed later. From the data shown in Table I the threshold energies for the different dissociation reactions can be calculated according to Eq. (3). The results are given in Table II. It is seen that all M_n clusters with $n=3,\ldots,8$ preferably dissociate by ejection of a dimer. Interestingly, the corresponding dissociation thresholds for dimer emission are all found to be within 5% of 2.1 eV regardless of cluster size. Hence, for larger clusters with $n>8$ we skipped the time-consuming determination of the most stable configuration and assumed $E_d(n>8)$ to be 2.1 eV. Since according to Sec. II the value of E_d was only used to distinguish between stable and unstable clusters, this assumption did not make any impact on the calculated results since no sputtered clusters with $n>8$ and internal energies less than 2.1 eV were detected.

B. Internal energy of ejected clusters before dissociation

In order to evaluate the fraction of metastables within the total flux of sputtered clusters, the internal energy distribution of the M_n clusters determined immediately after the ejection was calculated. As an example, the results obtained for trimers, tetramers, and pentamers ejected under 5-keV Ar^+ bombardment of a (111) metal surface are shown in Fig. 2. From these distributions, average internal energies of 2.9, 4.5, and 6.1 eV are calculated for sputtered M_3, M_4, and M_5 clusters, respectively. Within the statistical limitations, these values are found to be essentially independent of the primary-ion energy for the whole energy range studied. Moreover, no significant difference was found between the results obtained for the (111), (100), and (110) surfaces. From the distributions displayed in Fig. 2, it is found that around 80% of the trimers, 99% of the tetramers, and all of the clusters with $n\geq 5$ are unstable and will therefore dissociate during their passage away from the surface. Again, no significant variation of these numbers is found if the bombarding energy and/or the orientation of the bombarded surface is changed.

TABLE II. Threshold energies $E_{\rm th}^{(m)}$ for dissociation of M_n clusters into M_m and M_{n-m} fragments as evaluated from the EAM potential. Values are given in eV.

m	1	2	3	4
M_3	2.19			
M_4	2.42	1.98		
M_5	2.31	2.10		
M_6	2.41	2.09	2.32	
M_7	2.38	2.16	2.28	
M_8	2.24	1.99	2.21	2.10

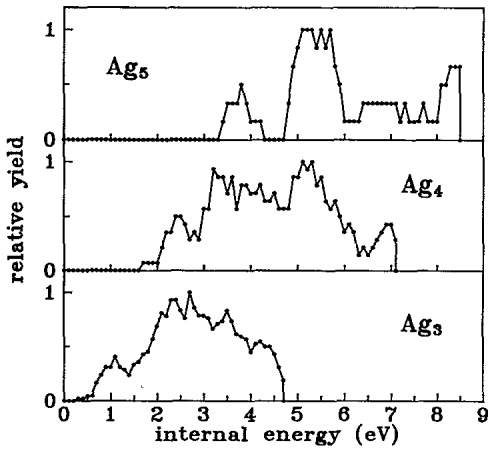

FIG. 2. Internal energy distribution of trimers (a), tetramers (b), and pentamers (c) ejected under 5-keV Ar^+ bombardment of a metal (111) surface as determined immediately after the ejection process.

C. Dissociation of unstable clusters

The next point of immediate interest concerns the time scale governing the dissociation of the metastable clusters. Therefore the dissociation lifetime, i.e., the time needed by an initial M_n cluster to dissociate into smaller (either stable or unstable) fragments, was calculated and averaged for all detected clusters of a given size n (regardless of the primary-ion energy or surface orientation used in the particular event which produced the cluster). Table III shows the resulting mean dissociation lifetime τ obtained for $n=3,\ldots,8$. The value given for M_3 must be regarded as a lower bound of τ since approximately 5% of the unstable trimers reached the upper integration time limit before dissociation and were thus counted at $\tau=200$ ps. It is seen from Table III that τ is largest for M_3 and decreases with increasing n. The only exception from this general trend is observed for M_6. It should be noted, however, that the dissociation of clusters is a statistical process and, hence, the total number of unstable clusters produced of a given size (included as "count" in Table III) needs to be large to obtain highly reliable values of τ. As a consequence, we consider the variation observed between M_5 and M_6 to be due to the statistical uncertainty of the average dissociation lifetime. For the same reason, the τ values obtained for clusters larger than M_8 were not considered to be statistically meaningful since only very few (below ten) clusters of each size were detected. Nevertheless, the corresponding values were calculated up to $n=31$ and were found to gradually decrease with increasing n. At a first glance, this behavior might be somewhat surprising since, due to the strongly increasing number of vibrational degrees of freedom with increasing cluster size, one would clearly expect longer lifetimes for larger clusters. This, however, only holds if the average internal energies $E_{\rm int}^{\rm av}$ of the different clusters were comparable. From the data

TABLE III. Internal energy $E_{\text{int}}^{\text{av}}$, dissociation lifetime τ, and total decomposition time t_d of unstable sputtered M_n clusters averaged over all clusters of a given size (regardless of the primary-ion energy and surface orientation used in the particular calculation which produced the cluster). For the definition of τ and t_d see text. The numbers given in the row labeled "count" denote the total number of clusters over which the average was performed.

n	3	4	5	6	7	8
Count	353	140	50	31	17	12
$E_{\text{int}}^{\text{av}}$ (eV)	2.9	4.5	6.1	7.9	8.5	10.9
τ (ps)	23	4.8	0.81	3.1	0.57	0.24
t_d (ps)	23	9	17	21	58	53

presented in Sec. III B we already know that this is not the case. Corresponding values of $E_{\text{int}}^{\text{av}}$ are also displayed in Table III. One finds that $E_{\text{int}}^{\text{av}}$ increases roughly proportional to the cluster size n, thus yielding an average internal energy per constituent atom of approximately 1.2 eV which is almost independent of the cluster size. If the mean dissociation lifetime is, for instance, estimated according to Rice-Ramsberger-Kassel (RRK) theory by inserting $E_{\text{int}}^{\text{av}}$ and E_d into the classical Kassel equation[42]

$$\tau_k = \left\{ A \left[1 - \frac{E_d}{E_{\text{int}}^{\text{av}}} \right]^{(s-1)} \right\}^{-1} \tag{4}$$

(with $s = 3n - 6$ being the number of vibrational modes in the molecule and A being a constant of the order of a vibrational frequency, i.e., $A \simeq 10^{13}$ s^{-1}), lifetimes of the order of a picosecond are calculated for all values of n between 3 and 8. Hence, even from this crude estimate it becomes understandable that τ does *not* increase dramatically with increasing n.

One major conclusion concerning the sputtering of small metal clusters can be immediately drawn from the results presented in Table III. The average lifetime of an ejected unstable M_n cluster is clearly below 100 ps, and for $n \geq 5$ even below 1 ps. In connection with the finding that virtually all M_n clusters with $n \geq 5$ are unstable, this means that a sputtered cluster of this size which has a typical center-of-mass velocity of 10^5 cm/s can travel only about 10 Å away from the surface before dissociation. The consequences are obvious. First, and probably most important, these clusters are practically not detectable by experiment. Second, regarding the fact that the dissociation time scale is comparable to the time scale of the sputtering process itself, we feel that these molecules should be considered as transient intermediate states of the particle ejection process rather than as metastable sputtering products.

An interesting question is how the mean dissociation lifetime of a sputtered cluster is related to its internal energy. In order to elucidate this point, the internal energy E_{int} of the molecules determined to be unstable was histogrammed into slots of $\Delta E_{\text{int}} = 0.5$ eV width and the mean lifetime τ was calculated separately for every slot. Due to the limited number of detected clusters with $n \geq 5$, this calculation was only performed for trimers and tetramers, since only in these cases the number of molecules contained in each slot was large enough (≥ 10) to determine a statistically meaningful value of τ. Figures 3 and 4 show the resulting plots which clearly indicate a strong correlation between τ and E_{int}. Due to the maximum integration time of 200 ps applied in the MD simulation (see Sec. II), the τ values given for the first slot immediately above the dissociation threshold represent lower limits. It is seen that the mean dissociation lifetime increases drastically with decreasing internal energy of the molecule. In order to try a more quantitative discussion, the trimer results presented in Fig. 3 were fit to the Kassel equation [Eq. (4)] yielding the fitting parameters $A = 1.3 \times 10^{14}$ s^{-1} and $s = 6.3$. While the value of A seems to be reasonable, the number determined for s is about twice as high as the actual number of vibrational degrees of freedom present in a trimer. This discrepancy is presumably due to the fact that the rotational excitation of the sputtered molecule which may significantly lower the effective dissociation threshold is not included in the Kassel theory. Although we are well aware that other quantum-mechanical theoretical approaches exist which are much more sophisticated than the simple RRK theory [for instance, Rice-Ramsberger-Kassel-Marcus (RRKM) theory (Ref. 42)] a quantitative comparison of the resulting expressions with our data would at least involve a detailed vibrational analysis of the molecule under investigation which is clearly beyond the scope of the present study.

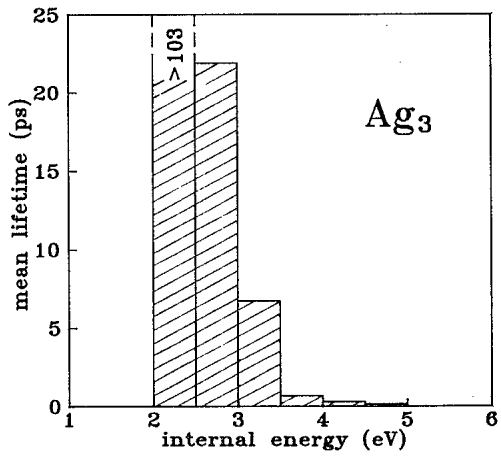

FIG. 3. Mean dissociation lifetime τ (i.e., time before dissociation into either stable or unstable fragments) vs the internal energy of sputtered metal trimers. The data was averaged over all trimers regardless of the primary-ion energy and/or surface used in the particular calculation which produced the cluster.

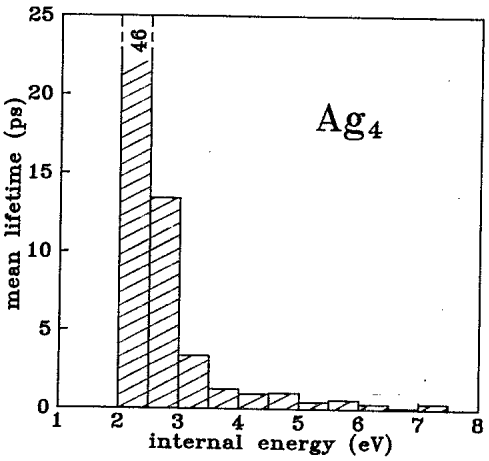

FIG. 4. Mean dissociation lifetime τ (i.e., time before dissociation into either stable or unstable fragments) vs the internal energy of sputtered metal tetramers. The data were averaged over all tetramers regardless of the primary-ion energy and/or surface used in the particular calculation which produced the cluster.

D. Decomposition into stable fragments

In order to evaluate the quality of the MD simulation, it is necessary to compare the calculated results with experimental data. As concluded in Sec. III C the only particles which are accessible experimentally are stable clusters and fragmentation products. As a consequence, in order to make such a comparison possible, the decomposition of sputtered unstable clusters has to be followed until only stable fragments remain. Figure 5 shows an example of such a complete decomposition pathway determined for an unstable M_{12} which was originally ejected from a (110) surface by a 1-keV Ar ion impact. In Fig. 5 the large number in the circle represents the size of the cluster, the small number written inside the circle the internal energy, and the one written above the circle the translational energy of a subcluster. The time value written below the circle denotes the time needed by the corresponding (sub)cluster to dissociate into the next set of subclusters. The particular example depicted in the figure was chosen since it illustrates most of the typical features which were generally observed: The larger agglomerates like the original M_{12} itself, the intermediate M_8 and the M_5 are very short lived and represent only transient stages of particle motion. The most abundant stable products obtained at the end of the fragmentation chain, on the other hand, are atoms, dimers, trimers and, in few cases, tetramers. It is also seen that an unstable tetramer is produced containing an internal energy which is only 0.6 eV above the dissociation threshold. The dissociation time τ needed by this tetramer is quite long and practically determines the total decomposition time $t_d \simeq 23$ ps of the original M_{12}. Table III shows a compilation of the averaged decomposition time t_d versus the cluster size n. Again, the value given for M_3 has to be considered as a lower bound. It is seen that t_d exhibits a completely different dependence on the cluster size than the corresponding dissociation lifetime τ. All values of t_d depicted in Table III have the same magnitude of several tens of picoseconds and, in contrast to the dissociation lifetime, a slight increase of t_d with increasing n is observed.

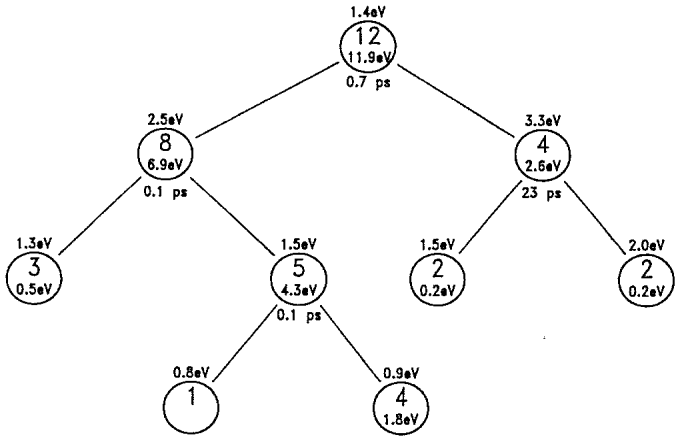

FIG. 5. Decomposition pathway of an unstable 12-mer ejected under bombardment of a metal (110) surface with 1-keV Ar^+ ions. Large numbers: Size n of subclusters; energy written inside and outside the circle: internal and translational energy of the subcluster; time: dissociation lifetime of the subclusters.

By following the decomposition pathway as described above for every cluster detected at the time when the MD simulation of the collision cascade leading to the sputter ejection of particles was stopped, the contribution of fragmentation to the yields of sputtered dimers, trimers, and tetramers can now be evaluated. As an arbitrarily chosen example, Table IV shows such a "fragmentation analysis" for the case of normally incident Ar^+ ions of 1 keV impinging onto a metal (111) surface. It is seen that, for instance, about 70% of the originally detected trimers are unstable and, hence, actually contribute to the *dimer* yield rather than to the trimer yield. If the decomposition of all unstable clusters is taken into account, the yields of stable dimers and trimers determined originally are both increased by approximately 30%. No stable clusters with $n \geq 4$ are produced with this particular combination of primary-ion energy and sample surface orientation. With increasing primary-ion energy, the influence of fragmentation on the yields of small clusters becomes even larger. For 5-keV Ar^+ ions impinging onto the (111) surface, the dimer and trimer yields are increased by 75% and 181%, respectively, and all stable tetramers which are detected result from fragmentation of larger clusters. As a consequence, we conclude that the unimolecular decomposition of larger clusters must under any circumstances be included into the analysis if the yields of sputtered multimers are to be predicted by MD simulations. Table V shows the resulting yields of stable silver dimers, trimers, and tetramers sputtered from a (111) surface by 5-keV Ar^+ ions. The particular primary-ion energy of 5 keV was chosen in order to compare the calculated yields with experimental data taken by electron-impact ionization of neutral Ag_n clusters

TABLE IV. Numbers of (stable and unstable) M_n clusters detected originally after the sputtering event and of stable products after complete decomposition of the unstable species. The results which are presented were taken from the calculation performed for Ar^+ ions of 1 keV normally incident on a metal (111) surface and represent an arbitrarily chosen example of a fragmentation analysis as described in the text.

Original cluster		Final decomposition products		
	Orig.	M	M_2	M_3
M_1	3369	3369		
M_2	369	0	369	
M_3	77	54	54	23
M_4	18	6	30	2
M_5	10	8	15	4
M_6	2	0	6	0
M_7	1	1	3	0
M_8	2	3	5	1
Total count		3441	482	30
Yield		3.44	0.48	0.03

sputtered from polycrystalline silver.[32] In order to allow a quantitative comparison with the experimental data, we determine from our calculation the ratio between the multimer yield and the yield of sputtered atoms by

$$[M_n]/[M]=\frac{Y_{M_n}}{Y_M}$$

(the determination of monomers is straightforward in the computer calculation). These values can now be compared with the corresponding experimental values which are also included in the table. It is seen that in particular the calculated $[M_3]/[M]$ and $[M_4]/[M]$ ratios are by approximately one order of magnitude higher than the corresponding experimental $[Ag_3]/[Ag]$ and $[Ag_4]/[Ag]$ values. This discrepancy is presumably due to the fact that the EAM potential overbinds the silver multimers (cf. Sec. III A). In order to estimate the significance of this effect, we determine the fraction γ of sputtered M_n multimers which are *spectroscopically* stable, i.e., which contain an internal energy less than the spectroscopic dissociation threshold E_d^s of the corresponding Ag_n cluster. For silver dimers and trimers, E_d^s can be calculated from the experimental atomization energies given by Hilpert and Gingerich[41] (see Table I). For silver tetramers, we are restricted to theoretical calculations of the atomization energy. Since according to Table I the experimental values for Ag_2 and Ag_3 are best approximated by the calculation of Bauschlicher, Langoff, and Partridge,[35] we take their value of the Ag_4 atomization energy and calculate dissociation thresholds of 1.66, 0.9, and 1.1 eV for Ag_2, Ag_3, and Ag_4, respectively. From these values, fractions γ of 81% for Ag_2, 21% for Ag_3, and 25% for Ag_4 were determined which were then used to correct the calculated M_n multimer yields. The resulting values are given in the row labeled "corr" in Table V. It is seen that the multimer to atom ratios determined from these values agree within factors of 1.6 (Ag_2) and 3.3 (Ag_3, Ag_4) with the experimental data. In particular, the drop by approximately one order of magnitude with every increase of the cluster size by one atom which is observed experimentally is now clearly reproduced by the MD simulation. It should be added that most recent experimental data on the yields of neutral

TABLE V. Total yields of M atoms and stable M_n clusters (including the fragmentation products of larger unstable clusters) ejected from a metal (111) surface bombarded by normally incident Ar^+ ions of 5 keV. In order to allow a quantitative comparison with experimental data obtained for Ag_n clusters sputtered from a polycrystalline silver surface (Ref. 32) (given in the last column), the calculated cluster yields have been corrected (rows labeled "corr") to account for the "overboundedness" of the Ag_n clusters by the EAM potential (see text).

Ejected particle	M	M_2	M_3	M_4
Calc. yield	5.273	1.204	0.135	0.008
Corr. yield	6.085	0.973	0.028	0.002
M_n/M calc.	1	22.8×10^{-2}	26×10^{-3}	15×10^{-4}
M_n/M corr.	1	16.0×10^{-2}	4.6×10^{-3}	3.3×10^{-4}
Ag_n/Ag expt.	1	10.2×10^{-2}	1.5×10^{-3}	1.0×10^{-4}

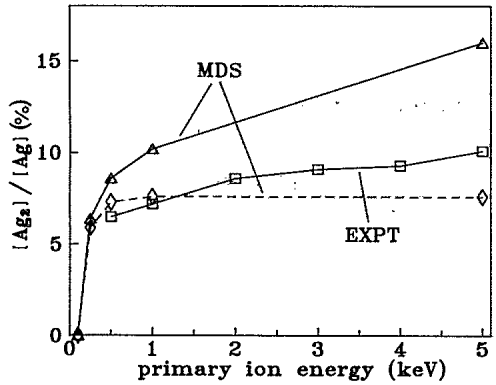

FIG. 6. Corrected dimer-to-atom ratio as evaluated from the MD simulation vs primary-ion energy for bombardment of a metal (111) surface with normally incident Ar^+ ions. Solid line: results including fragmentation of larger clusters; dashed line: results without including fragmentation. The line labeled "expt" represents experimental data obtained on a polycrystalline silver sample which was taken from Ref. 33.

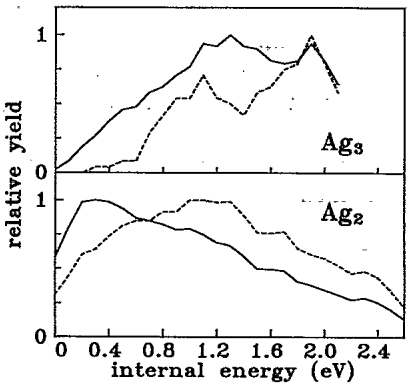

FIG. 7. Internal energy distribution of dimers and trimers sputtered from a metal (111) surface by normally incident Ar^+ ions of 5 keV. Solid line: all molecules including fragmentation products from unimolecular dissociation of unstable larger clusters; Dashed line: only the molecules which are detected immediately after the sputtering event.

Cu_n clusters sputtered from polycrystalline copper (detected by single-photon ionization) reveal essentially the same behavior.[43]

Another interesting point is given by the dependence of the dimer-to-atom ratio on the bombarding conditions present in the sputtering event. Figure 6 shows the corrected values of $[M_2]/[M]$ extracted from the simulation performed for the (111) surface versus the kinetic energy of the impinging primary Ar^+ ions. For comparison, corresponding experimental data obtained on a polycrystalline silver surface[33] are also included in the figure. It is apparent that apart from the fact that the MD results are by roughly a factor of 1.6 higher than the experimental values (see above), the experimentally observed variation of $[Ag_2]/[Ag]$ with the primary-ion energy is perfectly reproduced by the simulation. If, on the other hand, the contribution of fragmentation to the dimer yield is neglected, the dotted curve displayed in Fig. 6 is obtained from the simulation, i.e., no variation of $[M_2]/[M]$ with E_B would be expected above $E_B = 1$ keV. As a consequence, the increase of the dimer-to-atom ratio observed for $E_B \geq 1$ keV must be entirely attributed to the increasing role of unimolecular decomposition of larger clusters with increasing primary-ion energy.

E. Energy distributions

In view of the relatively large yield effects depicted in Sec. III D, it seems worthwhile to look for the contribution of unimolecular decomposition to the energy distributions of small sputtered clusters. As an example, Fig. 7 shows the distribution determined for the internal energy of dimers and trimers ejected under 5-keV Ar^+ bombardment of the (111) surface. In order to demonstrate the role of fragmentation processes, the distributions were evaluated either including (solid lines) or excluding (dashed lines) dissociation products. It is seen that in both cases the calculated internal energy distribution is shifted drastically towards lower energies if fragmentation is included into the analysis. Apparently the dimers and trimers produced by unimolecular decomposition of larger unstable species are relatively cold, i.e., contain on the average much less internal energy than those detected immediately after the ejection. Hence, in particular in cases where the contribution of fragmentation to the total yield of sputtered dimers and trimers is large (for instance, at high primary-ion energies), we also expect a significant decrease of the internal (vibrational and rotational) population temperature of the ejected molecules as predicted by MD simulations. A detailed investigation of this effect is planned to be the subject of a forthcoming paper.

Figure 8 shows the translational (center-of-mass) energy distribution evaluated for sputtered Ag_2 and Ag_3 molecules. Again, the data were plotted both including and excluding fragmentation. It is seen that also these curves are shifted towards lower energies if fragmentation prod-

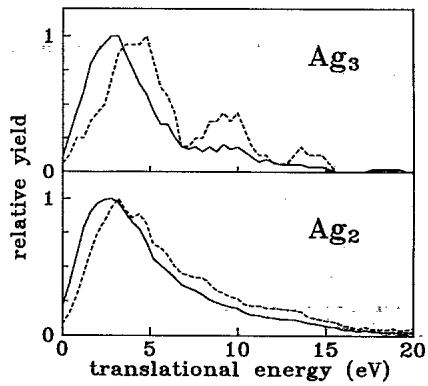

FIG. 8. Translational energy distribution of dimers and trimers sputtered from a metal (111) surface by normally incident Ar^+ ions of 5 keV. Solid line: all molecules including fragmentation products from unimolecular dissociation of unstable larger clusters; dashed line: only the molecules which are detected immediately after the sputtering event.

ucts are taken into account. This is particularly interesting since it removes a small discrepancy between calculated and experimental translational energy distributions of sputtered silver dimers which was encountered in our earlier work.[28]

IV. CONCLUSION

The sputtering of small homonuclear metal clusters M_n from single-crystal silver surfaces was studied by a molecular-dynamics simulation. The stability of such clusters as well as their fragmentation subsequent to the sputtering event was included into the MD treatment. It is shown that a significant fraction of sputtered metal dimers, trimers, and tetramers and virtually all sputtered multimers consisting of five or more atoms are unstable with respect to dissociation. The average time needed by such a cluster to decompose completely into stable fragments was determined to be of the order of 10 ps practically independent of the cluster size.

Since during this time the particles travel only about 100 Å away from the surface, it is concluded that these unstable clusters cannot be detected experimentally. Moreover, the mean dissociation lifetime of M_n clusters with $n \geq 5$ was found to be comparable to the duration of the collision cascade leading to the ejection of the sputtered particles itself. Hence, we suggest that these agglomerates detected in a molecular-dynamics simulation immediately after the trajectory integration is stopped should be considered as transient stages of the particle ejection process rather than as sputtered clusters. The yield of small clusters ($n=2$--4) is shown to be significantly increased by the fragmentation products originating from decomposing multimers, the effect becoming more pronounced with increasing primary-ion energy. The average internal and translational energy of stable products at the end of a fragmentation chain is found to be very low. Hence, the energy distributions of sputtered dimers, trimers, and tetramers can be markedly altered by fragmentation.

From the results presented in Sec. III, we conclude that the unimolecular decomposition of unstable multimers needs to be taken into account if yields, energy distributions, etc. of sputtered clusters are to be predicted theoretically. The present study shows that this is in principle feasible in a MD simulation by extending the trajectory integration to the dissociation of unstable sputtered species. By doing so, we feel that the fundamental problems concerning the theoretical description of cluster sputtering pointed out in Ref. 25 have been solved and the problem is brought back to the original limit, i.e., the quality of the interaction potential used.

ACKNOWLEDGMENTS

One of the authors (A.W.) greatly appreciates financial support from the Deutsche Forschungsgemeinschaft in the Sonderforschungsbereich 91. B.J.G. gratefully acknowledges support from the National Science Foundation, the Office of Naval Research, and the Camille and Henry Dreyfus Foundation. Penn State University and the University of Kaiserslautern supplied generous grants of computer time for this project.

[1]H. Oechsner, in *Physics of Ionized Gases 1984,* edited by M. Popovic and P. Krstic (World Scientific, Singapore, 1985), p. 571.
[2]H. M. Urbassek, Nucl. Instrum. Methods B **18**, 587 (1987).
[3]A. E. de Vries, Nucl. Instrum. Methods. B **27**, 173 (1987).
[4]W. Gerhard, Z. Phys. B **22**, 31 (1975).
[5]G. P. Können, A. Tip, and A. E. de Vries, Radiat. Eff. **21**, 269 (1974); **26**, 23 (1975).
[6]H. Oechsner, H. Schoof, and E. Stumpe, Surf. Sci. **76**, 343 (1978).
[7]R. A. Haring, H. E. Roosendaal, and P. C. Zalm, Nucl. Instrum. Methods B **28**, 205 (1987).
[8]R. Hoogerbrugge and P. G. Kistemaker, Nucl. Instrum. Methods B **21**, 37 (1987).
[9]K. J. Snowdon and R. A. Haring, Nucl. Instrum. Methods B **18**, 596 (1987).
[10]A. Wucher and H. Oechsner, Nucl. Instrum. Methods B **18**, 458 (1987).
[11]J. Dembowski, Thesis, University of Kaiserslautern, 1986.
[12]K. J. Snowdon, R. Hantschke, W. Heiland, and P. Hertel, Z. Phys. A **318**, 261 (1984).
[13]K. J. Snowdon, B. Willerding, and W. Heiland, Nucl. Instrum. Methods B **14**, 467 (1986).
[14]P. Sigmund, H. M. Urbassek, and D. Matagrano, Nucl. Instrum. Methods B **14**, 495 (1986).
[15]D. E. Harrison, Jr., and C. B. Delaplain, J. Appl. Phys. **47**, 2252 (1976).
[16]N. Winograd, D. E. Harrison, Jr., and B. J. Garrison, Surf. Sci. **78**, 467 (1978).
[17]B. J. Garrison, N. Winograd, and D. E. Harrison, Jr., J. Chem. Phys. **69**, 1440 (1978).
[18]B. J. Garrison, N. Winograd, and D. E. Harrison, Jr., Phys. Rev. B **18**, 6000 (1978).
[19]N. Winograd, K. E. Foley, B. J. Garrison, and D. E. Harrison, Jr., Phys. Lett. **73A**, 253 (1979).
[20]N. Winograd, B. J. Garrison, T. Fleisch, W. N. Delgass, and D. E. Harrison, Jr., J. Vac. Sci. Technol. **16**, 629 (1979).
[21]S. P. Holland, B. J. Garrison, and N. Winograd, Phys. Rev. Lett. **44**, 756 (1980).
[22]B. J. Garrison, J. Am. Chem. Soc. **102**, 6553 (1980).
[23]N. Winograd, B. J. Garrison, and D. E. Harrison, Jr., J. Chem. Phys. **73**, 3473 (1980).
[24]D. E. Harrison, Jr., P. Avouris, and R. Walkup, Nucl. Instrum. Methods B **18**, 349 (1987).
[25]H. H. Andersen, Nucl. Instrum. Methods B **18**, 321 (1987).
[26]B. J. Garrison, N. Winograd, D. M. Deaven, C. T. Reimann, D. Y. Lo, T. A. Tombrello, D. E. Harrison, Jr., and M. H. Shapiro, Phys. Rev. B **37**, 7197 (1988).
[27]A. Wucher and B. J. Garrison, Nucl. Instrum. Methods B **67**, 518 (1992).
[28]A. Wucher and B. J. Garrison, Surf. Sci. **260**, 257 (1992).
[29]D. E. Harrison, Jr., CRC Crit. Rev. Solid State Mater. Sci. **14**, 51 (1988).
[30]D. J. O'Connor and R. J. MacDonald, Radiat. Eff. **34**, 247 (1977).
[31]S. M. Foiles, M. I. Baskes, and M. S. Daw, Phys. Rev. B **33**,

7983 (1986).
[32]K. Franzreb, Thesis, University of Kaiserslautern, 1991.
[33]K. Franzreb, A. Wucher, and H. Oechsner, Fresenius J. Anal. Chem. **341**, 7 (1991).
[34]U. Röthlisberger and W. Andreoni, J. Chem. Phys. **94**, 8129 (1991).
[35]C. W. Bauschlicher, Jr., S. R. Langoff, and H. Partridge, J. Chem. Phys. **93**, 8133 (1990).
[36]J. Flad, G. Igel-Mann, H. Preuss, and H. Stoll, Chem. Phys. **90**, 257 (1984).
[37]H. Partridge, C. W. Bauschlicher, Jr., and S. R. Langoff, Chem. Phys. Lett. **175**, 531 (1990).
[38]K. Balasubramanian and P. Y. Feng, Chem. Phys. Lett. **159**, 452 (1989).
[39]S. Erkoc, Chem. Phys. Lett. **173**, 57 (1990).
[40]R. C. Baetzold, J. Chem. Phys. **68**, 555 (1978).
[41]K. Hilpert and K. A. Gingerich, Ber. Bunsenges. Phys. Chem. **84**, 739 (1980).
[42]P. R. Robinson and K. A. Holbrook, *Unimolecular Reactions* (Wiley, London, 1972).
[43]S. R. Coon, W. F. Calaway, J. W. Burnett, M. J. Pellin, D. M. Gruen, D. R. Spiegel, and J. M. White, Surf. Sci. **259**, 275 (1991).